Chapter 27

Rigid-Body Misalignment Parameters

Terrance J. Gaetz

In this chapter the incorporation of the rigid-body misalignment parameters into the raytrace model is discussed. In §27.1 the extraction of mirror rigid body parameters from the HATS optical data is discussed; in particular we are concerned with the focal plane image lateral parfocalization ("focal plane decenters") and the residual tilts. Other rigid body parameters are axial parfocalization (discussed in Chapter 26) and relative P to H decenters (*tilt-compensated decenters* (discussed in Chapter 30). The axial parfocalization was accommodated in the models by placing the mirrors at the as-measured positions and making a slight adjustment to the mirror maps. The remaining rigid body parameters were treated by adjusting the lateral position and tilts of the individual mirror elements; the construction of this rigid body database is described in §27.2. The database is based upon HATS measurements of the lateral parfocalization and residual tilt, and the X-ray measurements of the tilt-compensated decenters (Chapter 30).

27.1   HATS Data

During HRMA buildup, the alignment state of the HRMA optics was assessed using the Eastman Kodak Company HATS system (HRMA Alignment Test System). In the HATS tower configuration the HRMA optics were supported vertically in an assembly and testing tower (H optics upper, P optics lower) suspended above an optical flat (the Autocollimating Flat, or ACF); the configuration is illustrated schematically in Figure 27.1. An aperture mask with 24 evenly spaced apertures for each test zone (*i.e.*, mirror shell) was placed above the ACF. The aperture mask also carried a Tilt Reference Indicator (TRI, consisting of a pair of autocollimators, one looking down at the ACF, and the other looking up at a flat mounted in the CAP) which monitored the parallelism between the CAP and the ACF. HATS includes a Centroid Detector Assembly (CDA) mounted on rails at the top of the tower; this was used to assess the alignment of the optics at the 20 m (folded path) P focus or at the 10 m system focus. The alignment of the HRMA was probed using a double-pass system in which a directable laser beam from the CDA source (S) was reflected off an H, a P, the ACF, the P and H again, finally reaching the CDA detector (D); the centroids of the returned beam and an internal reference beam were measured using a quad-cell detector.

For a given mirror pair, the HATS measures the double-pass centroids for a set of 24 apertures equally spaced in azimuth around the optic. The alignment test is basically a double-pass Hartmann test of the X-ray optics. The test laser acts as a pencil beam probing a single azimuth (about the optical axis). The alignment state (and some low-order deformations of the optics) can be assessed
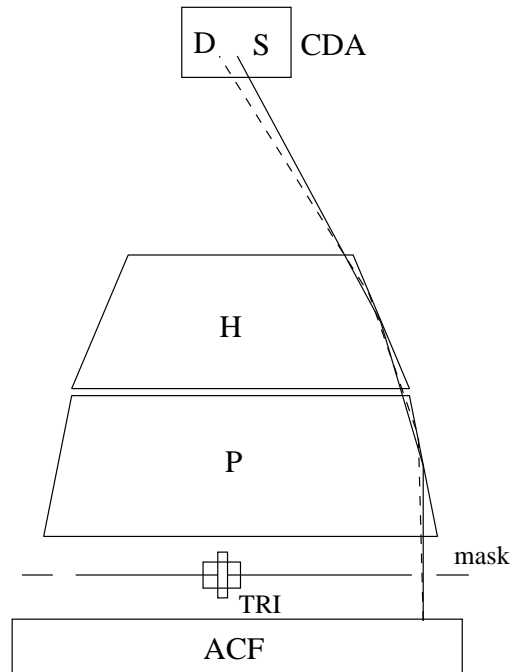
Figure 27.1: Schematic diagram of HATS double-pass configurations. A beam originates at source S, reflects from the H, the P, the Autocollimating Flat (ACF), the P and H again, and finally reaches detector D. The variation in the return beam centroid location with azimuth of the test beam provides information on mirror alignment.

by analyzing the variation in centroid location of the return beam as a function of the pointing azimuth. For example, if the CDA source/detector plane is in front of the HRMA focus (between the focus and the HRMA), the centroids will move along a defocus circle in phase with the beam azimuth (in-phase "1θ" variation). A relative tilt between the P and H, or a relative decenter between the optics produces coma which manifests as a "2θ" variation: the centroid position angle varies twice as quickly as the test beam azimuth varies. A lateral parfocalization error shows up as a relative displacement of the whole set of centroid positions; tilt and relative decenter can both change the lateral parfocalization.

These misalignment coefficients are clearly amenable to a Fourier analysis in which the appropriate low-order Fourier coefficients are interpreted in terms of misalignments. For a double-pass configuration containing both a P optic and its corresponding H optic, the coefficients relevant to rigid-body alignment are given in Table 27.1, in which Q_n is the Fourier coefficient of order n, and Re and Im indicate the real and imaginary components, respectively. The relations between the Fourier decomposition and HRMA alignment are described more fully in Lewis (1993).

Table 27.1: HATS Fourier Coefficients (ATP augmented data set)

Fourier Coefficient	Rigid Body Term
$Re(Q_0)$ and $Im(Q_0)$	lateral focus error
$Re(Q_1)$	axial focus error
$Re(Q_2)$ and $Im(Q_2)$	residual coma

Basically, Q_0 gives the displacement of the image in the focal plane, $Re(Q_1)$ gives the radius of the cone of rays (defocus circle, positive in front of the focal point, negative behind the focal point), and Q_2 provides the size and orientation of the 2θ coma circle. Because this is a double-pass experiment, the actual parfocalization and coma errors for a point source at infinity are a factor of two smaller than the Q_n coefficients. Although the interpretation of the HATS Q_0 and Q_2 Fourier coefficients is straightforward, the interpretation of Q_1 is complicated by a number of axially symmetric biases including deformation of the CAP under load, curvature of the ACF, "dimples" induced by the mirror supports under 1g, and refraction by radial temperature gradients within the HRMA.

27.1.1 November 1996 HATS ATP (Augmented) Data Set

The final HATS test data (Acceptance Test Procedure, or ATP) were obtained on November 9 and 10, 1996. We augment the original 9 ATP tests with an additional 15 tests performed at that time to obtain an augmented ATP data set as indicated in Table 27.2. We evaluated the means and standard deviations of the Fourier coefficients for this augmented test sequence; the Fourier coefficients evaluated and averaged using the SAO-written `PV-WAVE` package `hats_plot`. The means and errors used for the following analysis were taken from the output file `/ceaxaf1/ekc/HATS_data/hrma_atp/AZMIS.avg`; the errors quoted are the standard deviations of the set of Fourier coefficients obtained for the 24 individual alignment tests in the augmented HATS ATP data set. The Fourier coefficients relevant to rigid-body mirror element alignment are given in Table 27.3.

Table 27.2: HATS ATP (Augmented) Data

11/09/1996	21:49:36.000[†]	11/10/1996	07:35:05.000
11/09/1996	22:39:14.000[†]	11/10/1996	08:19:18.000
11/09/1996	23:44:28.000	11/10/1996	09:03:20.000[†]
11/10/1996	00:28:20.000[†]	11/10/1996	09:48:05.000[†]
11/10/1996	01:12:16.000[†]	11/10/1996	10:32:04.000[†]
11/10/1996	01:56:05.000[†]	11/10/1996	11:16:26.000[†]
11/10/1996	03:10:53.000	11/10/1996	12:00:32.000[†]
11/10/1996	03:54:49.000	11/10/1996	12:44:35.000[†]
11/10/1996	04:38:47.000	11/10/1996	13:28:30.000[†]
11/10/1996	05:22:45.000	11/10/1996	14:12:29.000[†]
11/10/1996	06:06:47.000	11/10/1996	14:56:24.000[†]
11/10/1996	06:50:54.000	11/10/1996	15:40:26.000[†]

[†]not in original HATS ATP data set

As noted above, the interpretation of Q_1 is complicated by a number of axially symmetric biases; see Chapter 26 for further discussion of axial parfocalization. The raytrace model for the axial parfocalization was updated by correcting the axial placements of the mirrors and adjusting the cone angles in the mirror maps; consequently the axial parfocalization is not discussed further here (see Chapter 26).

The HATS test procedure yields only relative values for the parfocalization so $\langle Q_0 \rangle = [-5.48, 9.42]$, the R^2-weighted mean, was subtracted from Q_0; R is an effective radius for the mirror pair and was taken from Waldman (1995). The resulting Q_n values are given in Table 27.4.

Relative rigid body misalignments of the P to H optics in either decenter or tilt can cause a

Table 27.3: HATS Fourier Coefficients

		units	MP1	MP3	MP4	MP6
1	$Re(Q_0)$	(μm)	-11.49 ± 9.42	-0.18 ± 9.40	-1.31 ± 9.66	-3.78 ± 9.24
2	$Im(Q_0)$	(μm)	7.62 ± 8.89	13.43 ± 8.77	9.89 ± 9.00	4.89 ± 9.08
3	$Re(Q_1)$	(μm)	-24.65 ± 1.09	-11.98 ± 2.42	-30.67 ± 1.35	6.81 ± 1.94
4	$Re(Q_2)$	(μm)	-8.66 ± 0.35	6.26 ± 0.58	5.76 ± 0.27	29.68 ± 0.62
5	$Im(Q_2)$	(μm)	2.60 ± 0.30	-1.93 ± 0.59	-0.76 ± 0.38	-3.07 ± 0.44

Table 27.4: HATS Fourier Coefficients: r^2-weighted Q_0 removed

		units	MP1	MP3	MP4	MP6
1	$Re(Q_0)$	(μm)	-5.97 ± 9.42	5.30 ± 9.40	4.17 ± 9.66	1.69 ± 9.24
2	$Im(Q_0)$	(μm)	-1.71 ± 8.89	4.10 ± 8.77	0.57 ± 9.00	-4.43 ± 9.08
3	$Re(Q_1)$	(μm)	-24.65 ± 1.09	-11.98 ± 2.42	-30.67 ± 1.35	6.81 ± 1.94
4	$Re(Q_2)$	(μm)	-8.66 ± 0.35	6.26 ± 0.58	5.76 ± 0.27	29.68 ± 0.62
5	$Im(Q_2)$	(μm)	2.60 ± 0.30	-1.93 ± 0.59	-0.76 ± 0.38	-3.07 ± 0.44

comatic image distortion in the focal plane. The coma circle diameter in the focal plane is related to a pure H relative decenter or a pure H relative tilt angle as:

	$1''$ H tilt	1 mm H decenter
Coma circle radius ($''$)	1	10
Coma circle radius (μm)	48.5	488

The breakdown between mirror element tilt and decenter is not uniquely determined by the coma as measured on-axis. Because both tilt and decenter introduce coma, the net coma can vanish for some combination movements; in particular, for combinations of H tilt + H decenter which are equivalent to a pure rotation about the H far focus, the comas introduced by the decenter and the tilt cancel each other leaving the net coma unchanged. We therefore factor the decenter and tilt into two components:

- coma; appears even on-axis
- tilt-compensated decenter; no on-axis coma, but an additional off-axis aberration appears (see Chapter 30).

We interpret the coma as a pure body-centered tilt of the H relative to its companion P optic. In the rest of this section, *tilt* refers to the corresponding component of on-axis coma expressed as a tilt of the H optic unless otherwise noted.

From the Q_0 and Q_2 coefficients it is straightforward to obtain the residual coma and lateral parfocalization:

Table 27.5:

$$
\begin{array}{rclcl}
\Delta X_{DPSAOsac} & = & +\Delta X_{SAOsac} & = & +Re(Q_0)/2 \\
\Delta Y_{DPSAOsac} & = & -\Delta Y_{SAOsac} & = & +Im(Q_0)/2 \\
azmis_{DPSAOsac} & = & -azmis_{SAOsac} & = & -Re(Q_2)/(2F_H) \\
elmis_{DPSAOsac} & = & +elmis_{SAOsac} & = & +Im(Q_2)/(2F_H)
\end{array}
$$

where $F_H = 9607$ mm is an effective focal length for HATS measurements (Waldman, 1995); the extra factors of 2 arise because this is a double-pass measurement. The numerical values for the lateral parfocalization and residual tilts are given in Table 27.6.

Table 27.6: Summary: HRMA Lateral Parfocalization and On-Axis Coma (SAOsac coordinates)

		units	MP1	MP3	MP4	MP6
Lateral Parfocalization	δX	(μm)	-3.00	$+2.65$	$+2.08$	$+0.84$
Lateral Parfocalization	δY	(μm)	$+0.86$	-2.05	-0.28	-2.22
On-Axis Coma	$elmis$	($''$)	$+0.02926$	-0.02069	-0.00423	-0.03292
On-Axis Coma	$azmis$	($''$)	-0.09019	$+0.06720$	$+0.06188$	$+0.31865$

27.1.2 Conversion of HATS data to Rigid Body Coefficients

On-Axis Coma: Tilt and Decenter

The coma measures a combination of relative P to H tilt and P to H decenter. As noted above, we decompose the mirror decenters and tilts into two components: pure body-centered H tilt, and a (coma-free) tilt-compensated H decenter. We assign all of the measured on-axis coma to a pure body-centered tilt; the tilt-compensated decenter is incorporated into the model in §27.2. When a body-centered tilt is applied to the H optic, the lateral focus position also shifts and this affects the lateral parfocalization. We restore lateral parfocalization to the measured values by applying a decenter to the mirror pair as a whole. In terms of the HATS Fourier coefficients, the corrected mirror pair body-centered decenter is given by in Table 27.7 where

$$Q_0' = Q_0 - Q_2^\star$$

and $\star$ indicates complex conjugate.

From these adjusted Q_0' and Q_2 values we derive the body-centered HATS-based decenter values (δX, δY) and tilts (`elmis`, `azmis`), in the `SAOsac` double-pass raytrace coordinates (see Tables 27.7 and 27.8). These can be converted from double-pass `SAOsac` to standard `SAOsac` coordinates using the relations in Chapter B; the results are given in Table 27.9.

27.2 Construction of the Mirror Rigid-Body Database

In this section we summarize the current rigid-body mirror database used as the basis for our raytrace models. We start with an ideal "OSAC"-style mirror prescription; the OSAC mirror conic

Table 27.7: Conversion to Rigid Body Misalignment

$\Delta X_{\mathrm{MP},DPSAOsac}$	$=$	$+\Delta X_{\mathrm{MP},SAOsac}$	$=$	$+Re(Q'_0)/2$
$\Delta Y_{\mathrm{MP},DPSAOsac}$	$=$	$-\Delta Y_{\mathrm{MP},SAOsac}$	$=$	$+Im(Q'_0)/2$
$azmis_{\mathrm{H},DPSAOsac}$	$=$	$-azmis_{\mathrm{H},SAOsac}$	$=$	$-Re(Q_2)/(2F_H)$
$elmis_{\mathrm{H},DPSAOsac}$	$=$	$+elmis_{\mathrm{H},SAOsac}$	$=$	$+Im(Q_2)/(2F_H)$

Table 27.8: Body-center rigid body coefficients (*double-pass* coordinate system)

Coefficient	units	MP1	MP3	MP4	MP6
$\delta X_{dp,P}$	(μm)	1.347	-0.482	-0.796	-13.995
$\delta Y_{dp,P}$	(μm)	0.446	1.087	-0.097	-3.748
$\mathrm{azmis}_{dp,P}$	($''$)	0.0	0.0	0.0	0.0
$\mathrm{elmis}_{dp,P}$	($''$)	0.0	0.0	0.0	0.0
$\delta X_{dp,H}$	(μm)	1.347	-0.482	-0.796	-13.995
$\delta Y_{dp,H}$	(μm)	0.446	1.087	-0.097	-3.748
$\mathrm{azmis}_{dp,H}$	($''$)	0.09019	-0.067200	-0.061875	-0.318647
$\mathrm{elmis}_{dp,H}$	($''$)	0.02926	-0.020686	-0.004233	-0.032918

is described by

$$r^2 = \rho_0^2 + 2Kz - Pz^2 \tag{27.1}$$

where r is the radius corresponding to location z along the axis; z is measured from the body center of the optic so ρ_0 is just the radius corresponding to the body center. The adopted mirror parameters, incorporating the effects of the end-cut, are given in Table 27.10 (Zhao, 1996).

To this we apply the decenters and tilts implied by the HATS optical measurements (Table 27.9), and the as-measured optic axial positions (see Chapter 26) to obtain Table 27.11. Recall that we are working in our standard `SAOsac` raytrace coordinate system so Z_0 is along the optical axis (positive *from* HRMA *towards* the detectors).

To this basic configuration we apply the optic-to-optic decenters as derived from the off-axis X-ray images (Chapter 30). The mirror (body-center) decenters must also be consistent with the optically determined (focal plane) decenters and coma. This was achieved as follows: A pure rigid body rotation of an H optic about its far focus preserves the coma in the focal plane. For ideal optics the distance from H body center to H far focus is 19668.11899 mm. Raytraces studies show that a tilt-compensated H decenter also shifts the focal plane centroid of the double-pass image by about 1.023902 times the magnitude of the relative H decenter; we can correct for this can be corrected by applying a compensating decenter of the mirror pair as a whole by an amount equal to $0.5 \times 1.023902 \times H_{\mathrm{decenter}}$. (The extra factor of 0.5 results because of the double-pass nature of the HATS alignment test.) That is, if the H to P decenter component of a tilt-compensated decenter of the H is $[\delta x_H, \delta y_H]$, the compensating tilt (in radians) is:

$$\delta elmis = -\frac{\delta y_H}{19668.11899}, \tag{27.2}$$

$$\delta azmis = -\frac{\delta x_H}{19668.11899} \tag{27.3}$$

and the compensating mirror *pair* decenter is $-0.5 \times 1.023902 \times [\delta x_H, \delta y_H]$.

In summary, the procedure for incorporating the P to H decenter is:

Table 27.9: Body-center rigid body coefficients (standard `SAOsac` coordinate system)

Coefficient	units	MP1	MP3	MP4	MP6
δX_P	(μm)	1.347	-0.482	-0.796	-13.995
δY_P	(μm)	-0.446	-1.087	0.097	3.748
azmis$_P$	($''$)	0.0	0.0	0.0	0.0
elmis$_P$	($''$)	0.0	0.0	0.0	0.0
δX_H	(μm)	1.347	-0.482	-0.796	-13.995
δY_H	(μm)	-0.446	-1.087	0.097	3.748
azmis$_H$	($''$)	-0.09019	0.067200	0.061875	0.318647
elmis$_H$	($''$)	0.02926	-0.020686	-0.004233	-0.032918

Table 27.10: `SAOsac` mirror parameters, baseline optic prescription

Mirror	P (dimensionless)	K (mm)	ρ_0 (mm)
p1	0.0	-8.9333113530131421	606.86080963697918
p3	0.0	-5.7939624154424676	488.46244215611011
p4	0.0	-4.5165799273846270	431.26225933154404
p6	0.0	-2.4957050467401789	320.56977725634789
h1	$-1.7797716637950735E\text{-}03$	-26.0506034413416841	579.89015840093919
h3	$-1.1532395834759916E\text{-}03$	-16.875942397594130	466.64379784205380
h4	$-8.9864417477996457E\text{-}04$	-13.150318066441841	411.91935912458604
h6	$-4.9625995845653374E\text{-}04$	-7.2620248152618760	306.09851668776219

1. Start with the baseline ideal optics prescription (Table 27.10).

2. Apply a mirror decenter/tilt combination which reproduces the optical measurements of the focal plane decenter and coma, and as-measured optic spacing (Table 27.11.)

3. Apply relative decenters to the H optics (Table 30.3).

4. Apply a compensating tilt to each H optic such that the combined decenter (Table 30.3) plus tilt is equivalent to a pure rotation of the H body center about the H far focus.

5. Decenter to the mirror pair as a whole by -1.023902 times half of the H decenter from Table 30.3 to restore lateral parfocalization.

The resulting rigid-body parameters are given in Table 27.12. These rigid-body data were incorporated into an updated raytrace mirror database; the current mirror database is `/proj/axaf/simul/databases/mirror/EKCHDOS06.rdb`. As noted in Chapter 26, the axial parfocalization correction was incorporated into the mirror maps by adjusting the mirror cone angles. The current HRMA model (`trace-shell4` configuration file, `xrcf_SAO1G+HDOS_HDOS-scat-970220_03`), incorporates the adjusted mirror maps.

The rigid-body configuration in Table 27.12 was converted into the `SAOsac` (double-pass) coordinate system using the transformations in Table B.2 and raytraced in a double-pass configuration; the optics were assumed to be otherwise ideal. The Fourier coefficients relevant to focal plane

Table 27.11: `SAOsac` mirror parameters, decenters and tilts from ATP data; as-measured axial mirror positions

Mirror	X_0 (mm)	Y_0 (mm)	Z_0 (mm)	azmis ($''$)	elmis ($''$)
P1	0.001347	−0.000446	−426.5761	0.0	0.0
P3	−0.000482	−0.001087	−436.7098	0.0	0.0
P4	−0.000796	0.000097	−440.3572	0.0	0.0
P6	−0.013995	0.003748	−445.0821	0.0	0.0
H1	0.001347	−0.000446	481.0146	−0.09019	0.02926
H3	−0.000482	−0.001087	480.9282	0.067200	−0.020686
H4	−0.000796	0.000097	480.8279	0.061875	−0.004233
H6	−0.013995	0.003748	479.2152	0.318647	−0.032918

Table 27.12: Rigid-Body Mirror Parameters (EKCHDOS06)

Mirror	X_0 (mm)	Y_0 (mm)	Z_0 (mm)	azmis ($''$)	elmis ($''$)
P1	0.1239	0.2151	−426.5761	0.0	0.0
P3	0.08675	0.2437	−436.7098	0.0	0.0
P4	0.08634	0.2168	−440.3572	0.0	0.0
P6	0.08625	0.2245	−445.0821	0.0	0.0
H1	−0.1154	−0.2060	481.0146	2.4194219	4.4454479
H3	−0.08365	−0.2345	480.9282	1.8542174	4.9943249
H4	−0.08386	−0.2065	480.8279	1.8468078	4.4350269
H6	−0.1096	−0.2067	479.2152	2.3720568	4.4891913

decenter and residual coma were evaluated and compared to the HATS-derived values given in Table 27.4; the resulting values are listed in Table 27.13. The values agree to better than $0.4\,\mu$m; this is satisfactory agreement, well within the measurement uncertainties for Q_0 and comparable to the measurement uncertainties for Q_2 (Table 27.3).

27.3   Future Directions

This is a preliminary assessment of the mirror rigid-body orientation parameters. As our data reductions and analyses are refined, the improved estimates of axial parfocalization (Chapter 26) and tilt-compensated decenters (Chapter 30) will be incorporated into the model.

The analysis of the optical alignment data can also be improved: various double-pass raytrace analyses were based on optics which were ideal other than for the misalignments. Because raytraces indicate that Fourier decomposition is insensitive to details of the mirror map (other than the axial parfocalization, as noted above), this is not expected to change the estimates appreciably.

Preliminary raytrace investigations indicate that the tilt-compensated decenters do not significantly bias the HATS-based measurements of the coma or parfocalization. It is possible that the tilt-compensated decenters affect some of the higher-order HATS residuals, though.

Finally, an assessment of the lateral parfocalization at XRCF needs to be made. Measurement

Table 27.13: Fourier Coefficients: HATS *vs.* raytrace

mirror	units	data	MP1	MP3	MP4	MP6
$Re(Q_0)$	(μm)	ATP Data	-5.9709	5.2962	4.1713	1.6929
$Re(Q_0)$	(μm)	raytrace	-5.6195	5.2857	4.1754	1.6076
$Re(Q_0)$	(μm)	residual	-0.3514	0.0105	-0.0041	0.0853
$Im(Q_0)$	(μm)	ATP Data	-1.7083	4.1013	0.5668	-4.4305
$Im(Q_0)$	(μm)	raytrace	-1.7612	4.1548	0.2073	-4.4666
$Im(Q_0)$	(μm)	residual	0.0529	-0.0535	0.3595	0.0361
$Re(Q_2)$	(μm)	ATP Data	-8.6649	6.2598	5.7638	29.6826
$Re(Q_2)$	(μm)	raytrace	-8.3901	6.2643	5.7719	29.6405
$Re(Q_2)$	(μm)	residual	-2.0748	-0.0045	-0.0081	0.0421
$Im(Q_2)$	(μm)	ATP Data	2.6014	-1.9269	-0.7608	-3.0664
$Im(Q_2)$	(μm)	raytrace	2.7256	-1.9222	-0.3803	-3.0516
$Im(Q_2)$	(μm)	residual	-0.1242	-0.0047	-0.3805	-0.0148

the lateral parfocalization in X-rays is complicated by several factors: tilts induced by 1g distortion of HRMA as supported in the horizontal XRCF configuration, maintaining stability and accuracy of absolute centroid positions over long timescales, and the large pinholes (10 μm or 20 μm). Although the X-ray measurements may not improve on the HATS values, the X-ray centroids will provide additional constraints on the 1g model. (In the optical HATS measurements the HRMA was supported vertically, so no appreciable 1g-induced tilts are introduced.)